International Journal of Computing and Digital Systems
2025, VOL. 17, NO.1, 1-10

http://dx.doi.org/10.12785/ijcds/1570999111

Detection of Soil Nitrogen Levels via Grayscale Conversion: A Full-Factorial Design of Experiment Approach

John Joshua F. Montañez[1,2]

[1]*College of Engineering, Bicol State College of Applied Sciences and Technology, Naga City, Camarines Sur, Philippines*
[2]*College of Engineering, Batangas State University, the National Engineering University, Batangas City, Philippines*

Received 16 February 2024, Revised 11 October 2024, Accepted 25 October 2024

Abstract: In smart agriculture, the detection of the level of soil nitrogen is essential in soil fertility and productivity that correlates to crop yields and fertilizer recommendations. With the advancement of technology, identification of such level is easily obtained using devices that capture images, which are affected by two factors, i.e., the tilting angle of the test tube and the lighting condition. The device produces images containing three colors, namely, red, green, and blue, respectively. Using grayscale conversion, these values are then converted into a single value to analyze appropriately. This study aims to determine the optimal combination of the factors to obtain the correct reading of Nitrogen using a full-factorial design of experiments with four replications designed by Minitab®; the design of the experiment is a valuable statistical tool that promotes efficient experimentations used by scientists and engineers. The results are analyzed using Analysis of Variance, and it is depicted that the determined factors, tilting angle and lighting condition, and their interactions are significant. The developed regression model explains 76.43% of variability among factors. The optimal setting for tilting angle is 90°, while the lighting condition should be indoors. Design of Experiment is a valuable statistical tool that promotes optimization and efficient experimentations used by scientists and engineers.

Keywords: Automation, Design of Experiments, Full-Factorial, Grayscale conversion. Nitrogen level, Optimization, RGB values

1. Introduction

From the modern global perspective, soil health and the management of soil nutrients have increased attention and have been the focus of research [1]. An urgent concern of each state government of ensuring sustainable and plentiful agricultural products and maintaining and promoting agricultural processes are undoubtedly needed to increase the food supply without compromising the health of the planet, considering that the population of the world continues to increase in number is notably observed [2].

The first of the primary macronutrients is Nitrogen, which is considered an essential component of nucleic acid and protein, which are the building blocks of plant cells. It is vital in the chlorophyll, which is included in photosynthesis, a process by which plants convert sunlight to helpful energy. Without Nitrogen, plants cannot produce necessary organic compounds for survival and growth [3]. Phosphorus is the second primary macronutrient for plants, necessary for transferring energy within the plant cells. It focuses on the growth and development of seeds and roots. Without Phosphorus, plants may show stunted growth, decreased seed production, and poor root development [4]. Potassium is the last of the primary macronutrients that regulate water balance since it maintains turgor pressure in plant cells. It also maintains the shape and prevents wilting. Without Potassium, no activation of vital enzymes will be possible [5].

Practices and guidelines on sustainable farming and implementation require monitoring and detecting levels of soil macronutrients (i.e., Nitrogen, Phosphorus, and Potassium) [6]. This permits information for farmers, agriculturists, and soil enthusiasts regarding future trends and application of the appropriate amount and type of fertilizers needed to ensure optimal plant growth and increased crop yield. This initiative not only assures increasing financial aspects as these reduce over and under-application of fertilizer, but it also aids in reducing any risk of environmental damage and degradation in soil fertility and productivity [7].

Moreover, monitoring and detecting soil macronutrients not only span agricultural production and the improvement of agricultural processes. Climate change, biodiversity, and water quality are all related to the maintenance of soil health [8]. Creating possible greenhouse gas that impacts climate change happens due to excessive application and imple-

E-mail address: jjfmontanez@astean.biscast.edu.ph

mentation of nitrogen-based fertilizers, which expel nitrous oxide into the atmosphere [9]. Any efforts to mitigate the effects of climate change must impart the principles and management of sustainable soil management to decrease greenhouse gas emissions [10].

Furthermore, overuse of fertilizer can cause unnecessary runoff into nearby water sources like rivers or oceans, negatively impacting aquatic ecosystems [11]. Excess phosphorous and Nitrogen from fertilizers may cause algal blooms in water bodies that consume oxygen and create dead zones in which aquatic living things cannot survive [12].

Soil Test Kits determine soil macronutrients that intend to analyze the given soil's characteristics and properties [13]. Planting crops, improving crop yields, and improving plant growth utilize this generally helpful produced information. The colorimetric approach states that soil test kits are considered cost-effective and time-efficient, making them a convenient tool for farmers, agriculturists, and interested individuals [14]. The colorimetric approach in the Soil Test Kits involves chemical reagents that change the color of the concentration and presence of specific soil components. Therefore, the color produced in the chemical process determines the corresponding level of the macronutrients present in the sampled soil [15].

With the recent advancement of technology, the colors produced by the reagents can be easily determined through image processing under computer vision without laboratory analysis, which is considered time-consuming and expensive; images capturing the colors the reagents produce are the main focus of image processing. This advancement allows us to analyze the nutrient content of the soil in a non-invasive or non-destructive way [16].

Several factors can affect the images produced, leading to an inappropriate reading of the levels of the soil macronutrients. These factors include user error, soil properties, and equipment calibration. However, the two significant factors affecting the reading results are the lighting condition and the tilting angles of the test tube containing the reagents [17].

The primary objective of this study is to determine the optimal lighting condition and tilting angles of the test tube, which will lead to the correct interpretation of the level of the soil macronutrients via an image produced from the chemical reagents. The objective can be achieved through the full-factorial design of experiments, which streamlines the process and saves time in soil nutrient analysis.

2. Related Literature and Studies

A. On the detection of Soil Macronutrients

The study of Isaak et al. [18] focuses on determining soil macronutrients through soil spectroscopy measurement, and its product was a device considered low-cost compared to laboratory-grade spectroscopy. The device observes the absorbance spectroscopy on the linear relationship in obtaining Nitrogen, Phosphorus, and Potassium through light-emitting diodes.

Yamin et al. [19] modified the colorimetric process for determining the macronutrients in oil palm plantations using the Soil Test Kit. The method describes the passage of light through an opaque medium utilizing a specified reagent in the soil solution. The study reported an accuracy of 91.7% for Nitrogen, 89.6% for Phosphorus, and 93.8% for Potassium. This research concluded with an Internet-of-Things network data fusion to assess the variation of soil macronutrients and the management of nutrients in oil palm plantations.

Kaushik [20] emphasized that in soil fertility and productivity, obtaining the soil characteristics, including the level of soil macronutrients, i.e., Nitrogen, Phosphorus, and Potassium, is vital, leading to food security. The study showcases the India-based soil macronutrient classification. Regarding the K-mean clustering method, India was divided into three clusters based on the absolute correlation values of various soil nitrogen, the different soil phosphorus content, and other organic carbon contents.

Patel et al. [21] incorporated hyperspectral remote sensing in determining and identifying soil Nitrogen, Phosphorus, and Potassium soil levels instead of laborious, cost-intensive, and time-consuming laboratory analysis. A derivative Analysis for the Spectral Unmixing approach was used to determine the composition of soil macronutrients. The study concluded with the fractional abundance of the soil macronutrients incorporated in situ to estimate soil fertility.

Sadowska, Świątkiewicz, and Żabiński [22] determined the soil macronutrients, i.e., Nitrogen and Potassium, in the three-year field trial on Peppermint (*Mentha piperita L.*) sandy soil. This is intended to determine the appropriate application of Biochar to plants and how it affects their growth. The main factors influencing the time-dependent responses of soil to Biochar were soil feedback, microbial, and plant. These were experimented with through a three-factorial design replicated three times.

Shiwakoti et al. [23] observed no difference in residue burning on soil macronutrients over time after the treatments incorporated in no burn residue incorporation with farmyard manure or pea vines, no burn or spring burn with the application of Nitrogen (0, 45, and 90 kg/ha), and fall burn wheat residue incorporation. The findings concluded that residue incorporation of farmyard manure at a fertilizer rate of Nitrogen at 90 kg/ha reduces the macronutrient decline over time.

Madhumathi, Arumuganathan, and Shruthi [24] conducted a study that incorporated a wireless sensor network that determines the level of soil pH, macronutrients, moisture, and temperatures and recommends an appropriate

amount of fertilizer and water to ensure optimal crop growth and yield. The monitoring indicators are projected on mobile applications from the cloud and wireless sensor networks. A system that can compete with existing time-consuming and cost-efficient laboratory analyses is what aims to be developed.

Burton, Jayachandran, and Bhansali [25] reviewed the related in situ soil nutrient monitoring research, including pH and soil macronutrients, i.e., Nitrogen, Phosphorus, and Potassium. The review study concluded that there is more to learn about the soil heterogeneity in several indicators of the electrochemical and optical system performance in situ. It further revealed that incorporating several sensors advances Internet-of-Things in agriculture is evident.

Lisuma, Mbega, and Ndakidemi [26] studied the effect of Tobacco (*Nicotiana tabacum L.*) plant in sandy soil, especially on the level of soil macronutrients and micronutrients, i.e., Calcium, Magnesium, and Sulfur at Tabora, Tanzania. Generally, the tobacco plant is expected to uptake soil macronutrients, and several experiments have compared the unfertilized and fertilized plants. The study concluded that there is a decrease in Potassium, Phosphorus, Sulfur, and Magnesium while there is a notable increase in Calcium and Nitrogen.

Alves et al. [27] developed an acceptable range for several vital macronutrients in plants, specifically the Forage cactus pear (*Opuntia ficus-indica Mill*). This range leads to appropriate nutrient content demands for soil management and improved fertilizer recommendations. The range is achieved using 4×3×2 factorial in randomized blocks in three replicates. Seventy-two plots were utilized for the macronutrient contents of dry matter and cladodes.

B. On the Use of the Design of Experiments

The study of Carvalho et al. [28] utilized the Design of Experiments to optimize collagen-chitosan-fucoidan cryogel manufacturing. The study's parameters or factors are fucoidan concentration, collagen concentration, and temperature. The Box-Behnken design was incorporated since it has three levels for three factors. According to the study, through the use of Design of Experiments, the optimal combination for the production of cryogels is 10% fucoidan, 5% of collagen, and 3% of chitosan at -80 C.

Outeiro et al. [29] implored the combination of machine learning and Design of Experiments to investigate the effects of the cutting conditions in the machining of Ti-6Al-4V Titanium Alloy. The objective of the research is to optimize the alloy's machinability while minimizing the residual stress time. The machine learning is intended to predict the residual stress versus the cutting conditions, i.e., cutting speed, uncut chip thickness, tool rake angle, and the cutting-edge radius incorporating linear regression. The results showcased that when there is a 40% increase in the residual stress at the machine surface, the rake angle must increase from negative (-6o) to positive (5o), and the cutting edge should be increased by 100% (from 16μm to 30μm) and the cutting speed must be decreased by 67% (from 60 to 20 m/min).

Dragan and Lelea [30] studied thermal design optimization through area reduction of printed circuit boards via the Design of Experiments under the optimization phase. Their study also mentioned that the shape of the printed circuit board is more vital than the area and how the said area was reduced in terms of the thermal performance of the experiments. The parameters were the length and width of the printed circuit board using the finite volume method. As the size of the printed circuit board decreases, the housing dimension is reduced while having the same thermal performance, leading to less integration space and lower costs.

Concrete mechanical properties prediction in the concrete mix design and the measurement of the concrete performance have been reviewed by Chong et al. [31] through the use of Design Experiments. Different waste materials, dosage and type of chemical additives, and amount and proportion of constituent materials were the different factors considered. The paper considered and reviewed several methods of analyzing concrete performance, namely, Artificial Neural Network, Response Surface Methodology, and Taguchi method. It positively criticized the Design of Experiments. It saves time and simplifies work without compromising mechanical performance.

Utilizing the Taguchi Design of Experiments, Chandra and Prakash [32] optimized the microchannel heat sink performance considering six factors, i.e., channel diameter, channel number, mass flux, channel length, power, and time. Optimizing the factors mentioned above while minimizing the surface temperature of experimental results was its main purpose. The optimized flux (150kg/m2s) and the higher number of channels (13) are vital in the heat transfer performance of the microchannel heat sink.

Arcieri, Baragetti, and Ž. Božić [33] used the Design of Experiments to determine which among the parameters highly influenced the residual stress distribution in an hourglass specimen subjected to the impact of a foreign object damage on 7075-T6; the 7075-T6 is an alloy in the aeronautical industry. The specimen was tested with bending or axial fatigue load and was assessed using finite element analysis. It resulted in incorporating high-impact forces that observe high tensile stresses, which are unfavorable from a fatigue point of view, and hence, it is wanted to have a low weight and reduce speed.

In the study of Guerra-Zubiaga, and Luong [34], the energy consumption of industrial robots is aligned with the objectives of Industry 4.0, i.e., reduced energy consumption, utilizing the Design of Experiments. The observed factors are temperature, payload, speed, and acceleration, using the linear factorial experiment analysis. The study observed that the most contributing factors to industrial

robots' increased energy consumption are linear speed and acceleration, having a percentage of 95% in the first three joints of a Kawasaki robot.

According to the literature review conducted by Román-Ramírez and Marco [35], in optimizing the development of lithium-ion batteries, the Design of Experiments played an essential role in observing time-saving initiatives and cost-reduction measures in the production of the batteries, as mentioned above. Several factors were considered depending on the objectives of various researchers, including ageing electrode formulation, active material synthesis, thermal design, capacity, and charging.

Yarici and Öztürk [36] analyzed the inverted square split ring resonator in terms of its resonance frequencies based on the chosen geometric parameters, using the Design of Experiments approach. The distance between the rings, the width of the rings, and the split width of the rings were investigated and considered as the factors, while the interaction in terms of the frequencies produced is the response of the study. The conclusion focused on the most significant parameter, the distance between rings and the width of the rings, while the least significant is the split width of the rings.

Rodriguez et al. [37] simulated the texture geometries in optimizing tribological properties in terms of surface texturing via Design of Experiments- Box Behnken. The study factors are the percentage of the textured area, depth, width, and oil film thickness. Texturing reduced the Coefficient of Friction in the Tribological tests and aided in the consumption of laboratory resources. The study mentioned that while all factors are significant, the lubricant film thickness is statistically significant.

C. On the determined factors for the Design of Experiments

Dacay et al. [38] developed a mobile application that determines the Nitrogen, Phosphorus, and Potassium of soil dedicated to corn. The study incorporated an optical transducer, which is considered a wavelength detection sensor that needs a light-emitting diode as a light source. The study results were able to detect the soil macronutrients and were validated by the Department of Agriculture-Soil Laboratory.

Manickam [39] crafted a framework for monitoring the soil condition using the Internet of Things. The study incorporated several sensors, namely pH value, humidity, moisture, temperature, and light, which were attributed to the increase in crop production. The data from the sensors were sent to MCP3204 ADC and from ADC to the cloud via Raspberry Pi.

Golicz et al. [40] investigated the potential employment of a smartphone application alongside Nitrogen and phosphate-sensitive test strips intended to determine the content of plants available found in the soil. The noted errors in determining soil nutrients were attributed to temperature dependency, chemical interferences, and ensuring optimal light conditions.

Lavanya, Rani, and GaneshKumar [41] presented a study focusing on the Internet of Things that incorporated Nitrogen, Phosphorus, and Potassium sensors in conjunction with light-dependent resistors and light-emitting diodes. An optimal light condition is vital in increasing the farmer's yields. Collected data are then sent to the Google Cloud database for a fast retrieval system that includes fuzzification of the levels of the soil macronutrients.

Hou et al. [42] studied the additive effect of biochar amendment nitrogen deposition that stimulates plant growth, photosynthesis, and Nitrogen, Phosphorus, and Potassium observance. In determining the photosynthetic gas exchange, being packed under good light conditions is one of the criteria for choosing mature fresh leaves for measures.

Budinski and Donlagic [43] incorporated colorimetric chemical sensing into the fluidic flow injection sensor system. The study's sensor system description mentioned that the fiber end face must be substantially titled; an extreme tilt angle also decreases the amount of returned light signal. The angle between 9° and 10° allowed a back reflection from the microcell's end cap.

Yuan et al. [44] mentioned that the titling angle is vital for achieving the minimum separation time and maximum plasma volume with high purity in developing manual and portable centrifuges for myocardial infarction diagnosis. Upon tilting the angle and tuning the diameter of the blood sample vessel, 99.9% purity plasma was observed in less than 3 min.

Guterstam et al. [45] presented a portion of their study regarding the critical tilt angle affecting the implicit model of other people's visual attention. It was considered an invisible force-carrying beam projecting from the eyes. Several experiments were conducted to confirm the study's claims. The respondents' judgment was highly affected by the image of a face to one side and staring at the object.

Huang et al. [46] studied how to determine the optical rotation of liquid crystal polymer retarders using digital image processing. The study mentioned an optimal optical rotation angle or tilting angle ranging from -90° to 90° for two opposing wedge-shaped dark areas by computation of the titling angle, optimization of the detection speed, and more substantial stability of the mechanical properties of the crystal polymer vortex retarder.

Yukhymenko et al. [47] studied a multistage shelf device using a fluidized bed for heat-mass transfer processes. In the processes mentioned in the study, the optimal angle of the shelve is 25° concerning the horizontal. This means that material particles on the shelf surface have a smaller angle, impeding the material particle's free flow concerning the

TABLE I. Factors and Their Levels

Factor	Low(-1)	High (+1)
Tilting Angle	45°	90°
Lighting Condition	Indoor	Outdoor

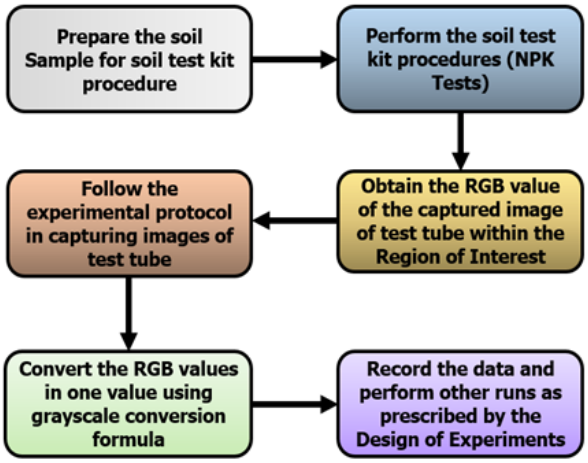

Figure 1. Procedural Flowchart

outloading space.

3. Methodology

This section discusses the various strategies and techniques for achieving the research objectives. It must outline the series of instructions to be observed to be systematic and thorough in executing the experimental protocols. The essence of establishing the design of the experiment is tantamount to yielding reliable and accurate results, emphasizing suitable statistical tools for analysis, and leading to the likelihood of producing valuable insights among factors.

A. Procedural Flowchart

Figure 1 showcases the procedural flowchart of the study, composed of six significant steps to fulfill the research objectives. Following the correct soil sampling for the soil test kit is vital in detecting soil macronutrients. The soil sample must be collected, and the correct representation of the tested area must be observed. After the soil has been successfully sampled, it is ready to be tested in terms of the procedure set by the soil test kit, which performs the nitrogen and phosphorus tests.

This produces several test tubes that have reagents with their corresponding color. The soil test kit observes the colorimetric method, pinpointing the level of the soil's macronutrients. Capturing the test tubes containing reagents is necessary at this point, as mentioned above, to determine their RGB values that directly link to the level of soil macronutrients being tested at hand. Observing the experimental protocol proves crucial mainly because experimentation observes the full-factorial design of experiments that lessen the number of runs, making gathering necessary data efficient and time-saving.

B. Selection of Factors

The corresponding RGB values shall be extracted and analyzed appropriately using the device that captures the images from the test tube with reagents that have set a region of interest. The grayscale conversion formula is imperative to convert the necessary three-value factors, i.e., Red Value, Green Value, and Blue Value, into a single response. As a prelude to the statistical treatment of the data, necessary responses shall be recorded. The runs must be precisely executed, ensuring consistency and replicability, making the results reliable and accurate as carefully prescribed by the Design of Experiments.

It is crucial to determine the factors that affect the system's output before optimizing the system and conducting experiments. In line with the related literature and studies, the tilting angle of the test is one of the identified factors in detecting soil macronutrients. tubes containing the reagents and the lighting conditions where the images were captured.

These factors are chosen so that the levels are lowest and highest. Table 1 summarizes the factors and their corresponding levels. The tilting angle has two levels, 45° and 90°, while the lighting condition has two environments, outdoor and indoor. This experimental protocol ensures the reliability and accuracy of the study's results.

C. Full factorial design of experiments using Minitab®

Implementing the full factorial design can be done using Minitab®, a high-performance statistical software package that is widely used in data analysis, quality control, and especially in designing Experiments used by industry practitioners and engineers. The software offers various designs, including factorial response surface and mixture designs.

In this study, the design matrix was designed by Minitab®, considering 2^2 full-factorial designs of experiments under four replications. Table 2 summarizes the runs that the research must follow in the experimentation, leading to the time-saving and cost-effective gathering of necessary data. Sixteen runs must be completed for the analysis to be possible. In the Minitab® graphical user interface, the factors can be coded or uncoded depending on the user's appreciation.

D. Grayscale Conversion of RGB Values

The standard color model utilized in digital images is RGB (Red, Green, Blue) values, representing the three

TABLE II. Response Matrix for Four Replicates

Run	Titling Angle	Lighting Condition	Grayscale Values
1	45°	Indoor (-1)	126.11
2	90°	Indoor (-1)	190.13
3	45°	Outdoor (+1)	128.07
4	90°	Outdoor (+1)	89.51
5	45°	Indoor (-1)	126.81
6	90°	Indoor (-1)	157.99
7	45°	Outdoor (+1)	126.18
8	90°	Outdoor (+1)	126.34
9	45°	Indoor (-1)	125.31
10	90°	Indoor (-1)	182.60
11	45°	Outdoor (+1)	109.90
12	90°	Outdoor (+1)	93.51
13	45°	Indoor (-1)	99.20
14	90°	Indoor (-1)	158.32
15	45°	Outdoor (+1)	108.17
16	90°	Outdoor (+1)	106.18

primary colors with individual pixel values from 0 to 255.

In this study, the device that captures the images of the test tubes contains the chemical reagents that produce an RGB value, which has three individual values for red, green, and blue. It is essential to convert these three values to a single value, making it a single channel of information for easy processing and analysis in the design of experiments. There are many ways to convert the RGB values into grayscale, and this includes the lightness method, the average method, and the luminosity method [47], [48], [49], [50]. The formula for the luminosity method is shown in formula (1) below; this converts RGB values to grayscale values:

$$Grayscale = 0.3R + 0.59G + 0.11B \quad (1)$$

4. Results and Discussion

This section discusses the study's results after it underwent the processes set forth by the procedural flowchart found in the methodology section. The Design of Experiment was followed as prescribed by the design matrix. The data collected gathered were analyzed using Minitab®.

A. Data Gathering of Grayscale Values

Table 2 summarizes the results of the 16 runs designed by Minitab® according to a 2^2 full factorial design of experiments with four replicates. The RGB values were initially recorded and computed accordingly using formula (1) to convert the RGB values into grayscale values. Upon having a single value, this was recorded in Table 1 and was ready to be analyzed by Minitab®.

B. Significance of Effects

The significance of the effects, with $\alpha = 0.05$, can be determined by comparing the effects' computed p-value and its interaction. Table 3 summarizes the coded coefficients containing valuable values like the computed p-values

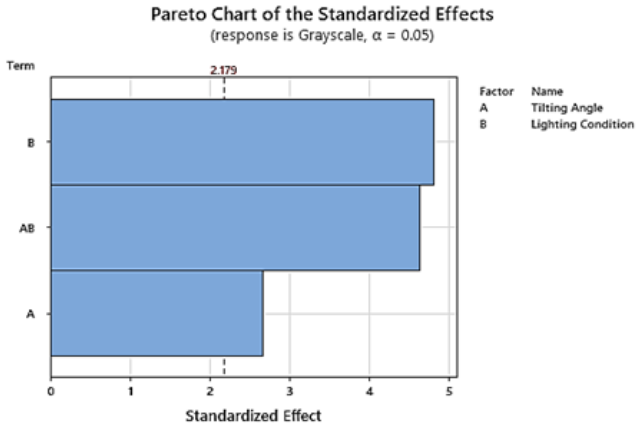

Figure 2. Pareto Chart of the Standard Effects

of tilting angle, lighting condition, and their interaction through using Minitab® as a computer-aided software for statistics.

Analyzing Table 3 and the Pareto chart of the standardized in Figure 2 shows that all the effects and their interactions are significant since all of them are less than 0.05, with values of 0.020 for tilting angle, 0.000 for lighting condition, and 0.001 for tilting angle*lighting condition. In Figure 2, the tilting angle, lighting condition, and titling angle*lighting condition crossed the dotted red line, concluding its significance in the model.

Table 3 also indicates the value for the variance inflation factor (VIF), which primarily concerns measuring the extent to which the factors are influenced or inflated. This assesses the amount of multicollinearity present in the developed regression model. In the final analysis, no multicollinearity is present in the developed regression model following the

TABLE III. Coded Coefficients

Term	Effect	Coef	SE Coef	T-Value	P-Value	VIF
Constant		128.40	3.62	35.45	0.000	
Titling Angle	19.35	9.68	3.62	2.67	0.020	1.00
Lighting Condition	-34.83	-17.41	3.62	-4.81	0.000	1.00
Titling Angle*Lighting Condition	-35.55	-16.77	3.62	-4.63	0.001	1.00

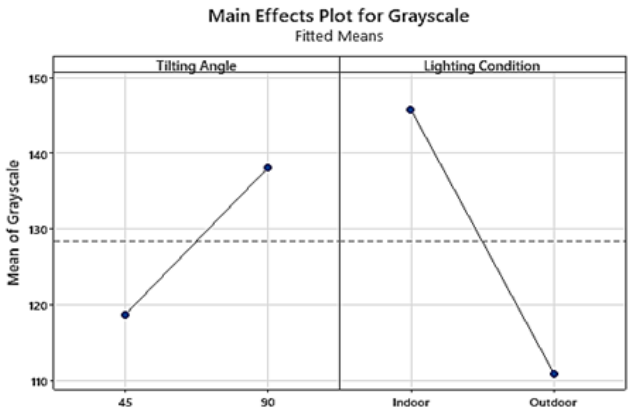

Figure 3. Main Effects Plot for Grayscale with Titling Angle and Lighting Condition as Factors

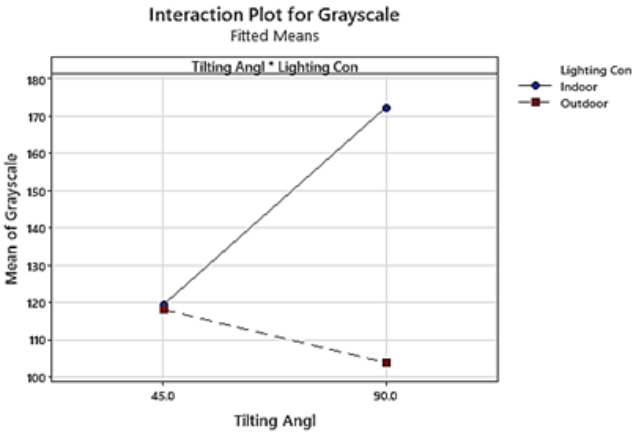

Figure 4. Interaction Plot for Grayscale intended for Tilting Angle and Lighting Condition

factors and their interaction having a VIF of less than 10.

C. Regression Model

After performing the needed runs and experimentations, they concluded a statistically reliable and helpful model primarily based on Analysis of Variance. The developed model is found in formula (2), calculated by Minitab®. A need to reconstruct the model by omitting insignificant factors or interactions is unnecessary since Table 3 concluded that all the factors and their interaction are significant.

$$Grayscale = 99.4 + 0.430TA + 32.9LC - 0.746TA * LC \quad (2)$$

where TA is the tilting angle, LC is the lighting condition.

The developed regression models' characteristics (S = 14.4954, R^2 = 81.15%, R^2(adj) = 76.43%, R^2(pred) = 66.48%) based on the factors and their interaction. The R^2 explains the proportion of the entire variability of the developed model, and the computed R^2 is 81.15%. However, R^2 is easily threatened by the increase of factors, even by the increase of insignificant factors. Thus, the other parameter, R^2 is useful since it is adapted to the total model size and thus explains 76.43% of the variability in the incoming new data.

D. Main Effects and Interaction Plots

The combined main effects plot for the titling angle and lighting condition is found in Figure 3. When comparing the main effects of tilting angle and lighting condition, the light condition has a dominant effect in the regression model compared to the titling. There is an increase in grayscale value as the tilting angle is changed from 45°to 90°, while there is a decrease in grayscale value once the test tube is placed from indoor to outdoor. Since the tilting angle and lighting condition are significant, it is necessary to check the interaction between the tilting angle and lighting condition.

Figure 4 showcases the interaction of tilting angle and lighting conditions. The tilting angle and lighting condition have significant interaction as the two lines do not exhibit a similar line behavior. Therefore, having different slopes indicating an intersection in the lines is a means of verification.

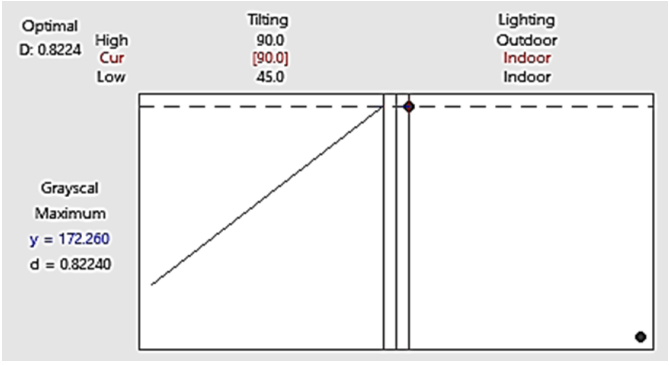

Figure 5. Optimization chart for the Grayscale Values

TABLE IV. Multiple Response Prediction

Variable	**Setting**			
Titling Angle	90°			
Lighting Condition	Indoor			
Response	**Fit**	**SE Fit**	**95% CI**	**95% PI**
Grayscale	172.26	7.25	(156.5, 188.1)	(137.0, 207.6)

E. Optimizing the factors

To optimize the factors by giving the appropriate RGB values and then converted to a grayscale value, the Minitab® can determine the optimal combination and values of the factors. Table 4 and Figure 5 summarize and depict the optimal tilting angle and lighting condition values. The optimal tilting angle should be 90°, and the optimal lighting condition should be indoors under a 95% confidence interval between 156.5 and 188.1 and a 95% prediction interval between 137.0 and 207.6.

5. Conclusion

The Design of Experiments explores the logical combination of factors governed by the titling angle and lighting condition for the grayscale values. Thus, its utilization in the optimization of the appropriate determination of the levels of soil nitrogen is substantially beneficial. The exploration of the interaction of the factors was allowed by it as well. The optimization process is geared towards enhanced accuracy and precision in the analysis, improved overall quality, and time-saving and cost-efficient experimentation. Furthermore, the success of using the Design of Experiments depends on the appropriateness of the experimental protocol, the data quality, and the accurate interpretation of results. They are using Minitab® as computer-aided software that allows scientists and engineers to efficiently explore the factors and their corresponding interactions, thus allowing them to determine the optimal conditions and combinations of factors effectively.

References

[1] U. D. Corato, "Towards new soil management strategies for improving soil quality and ecosystem services in sustainable agriculture: Editorial overview," *Sustainability*, vol. 12, no. 22, p. 9398, 2020, doi: 10.3390/su12229398.

[2] E. Workie, J. Mackolil, J. Nyika, and S. Ramadas, "Deciphering the impact of covid-19 pandemic on food security, agriculture, and livelihoods: A review of the evidence from developing countries," *Current Research in Environmental Sustainability*, vol. 2, p. 100014, 2020, doi: 10.1016/j.crsust.2020.100014.

[3] R. K. Tewari, N. Yadav, R. Gupta, and P. Kumar, "Oxidative stress under macronutrient deficiency in plants," *Journal of Soil Science and Plant Nutrition*, vol. 21, pp. 832–859, 2021, doi:10.1007/s42729-020-00405-9.

[4] M. J. Hawkesford *et al.*, "Functions of macronutrients," in *Marschner's Mineral Nutrition of Plants (Fourth Edition)*. Academic Press, 2023, pp. 201–281, doi: 10.1016/B978–0–12–819 773–8.00 019–8.

[5] R. Khalil, N. Elsayed, T. A. Khan, and M. Yusuf, "Potassium: A potent modulator of plant responses under changing environment," in *Role of Potassium in Abiotic Stress*, 2022, pp. 221–247, doi:10.1007/978 981–16–4461–0_11.

[6] A. Pal, S. K. Dubey, and S. Goel, "Iot enabled microfluidic colorimetric detection platform for continuous monitoring of nitrite and phosphate in soil," *Computers and Electronics in Agriculture*, vol. 195, p. 106856, 2022, doi:10.1016/j.compag.2022.106856.

[7] G. Prabakaran, D. Vaithiyanathan, and M. Ganesan, "Fpga based effective agriculture productivity prediction system using fuzzy support vector machine," *Mathematics and Computers in Simulation*, vol. 185, pp. 1–16, 2021, doi:10.1016/j.matcom.2020.12.011.

[8] B. Kashyap and R. Kumar, "Sensing methodologies in agriculture for soil moisture and nutrient monitoring," *IEEE Access*, vol. 9, pp. 14 095–14 121, 2021, doi:10.1109/ACCESS.2021.3052478.

[9] T. Allsop and R. Neal, "A review: Application and implementation of optic fibre sensors for gas detection," *Sensors*, vol. 21, no. 20, p. 6755, 2021, doi:10.3390/s21206755.

[10] G. S. Malhi, M. Kaur, and P. Kaushik, "Impact of climate change on agriculture and its mitigation strategies: A review," *Sustainability*, vol. 13, no. 3, p. 1318, 2021, doi:10.3390/su13031318.

[11] B. Sarker, K. N. Keya, F. I. Mahir, K. M. Nahiun, S. Shahida, and R. A. Khan, "Surface and ground water pollution: causes and effects of urbanization and industrialization in south asia," *Scientific Review*, vol. 7, no. 3, pp. 32–41, 2021, doi:10.32861/sr.73.42.49.

[12] A. Bailey, L. Meyer, N. Pettingell, M. Macie, and J. Korstad, "Agricultural practices contributing to aquatic dead zones," in *Ecological and Practical Applications for Sustainable Agriculture*, K. Bauddh, S. Kumar, R. Singh, and J. Korstad, Eds. Springer, 2020, doi:10.1007/978-981-15-3372-3_17.

[13] M. Tobiszewski and C. Vakh, "Analytical applications of smartphones for agricultural soil analysis," *Anal Bioanal Chem*, 2023, doi:10.1007/s00216-023-04558-1.

[14] H. Yin, Y. Cao, B. Marelli, X. Zeng, A. J. Mason, and C. Cao, "Soil sensors and plant wearables for smart and precision agriculture," *Advanced Materials*, vol. 33, no. 20, p. 2007764, 2021, doi:10.1002/adma.202007764.

[15] G. V. de Mello Gabriel, L. M. Pitombo, L. M. T. Rosa *et al.*, "The environmental importance of iron speciation in soils: evaluation of classic methodologies," *Environ Monit Assess*, vol. 193, p. 63, 2021, doi:10.1007/s10661-021-08874-w.

[16] M. Modzelewska-Kapituła and S. Jun, "The application of computer vision systems in meat science and industry – a review," *Meat Science*, vol. 192, p. 108904, 2022, doi:10.1016/j.meatsci.2022.108904.

[17] G. Shura, H. M. Beshir, and A. Haile, "Improving onion productivity

through optimum and economical use of soil macronutrients in central rift valley of ethiopia," *Journal of Agriculture and Food Research*, vol. 9, p. 100321, 2022, doi:10.1016/j.jafr.2022.100321.

[18] S. Isaak, Y. Yusof, N. H. Ngajikin, N. Ramli, and C. M. Wen, "A low cost spectroscopy with raspberry pi for soil macronutrient monitoring," *TELKOMNIKA (Telecommunication Computing Electronics and Control)*, vol. 17, no. 4, pp. 1867–1873, Aug 2019, doi: 10.12928/telkomnika.v17i4.12775.

[19] M. Yamin, W. I. W. Ismail, M. S. M. Kassim, S. B. A. Aziz, F. N. Akbar, R. R. Shamshiri, M. Ibrahim, and B. Mahns, "Modification of colorimetric method based digital soil test kit for determination of macronutrients in oil palm plantation," in *Proc. of the 2020 IEEE 7th International Conference on Smart Instrumentation, Measurement and Applications (ICSIMA)*, Nov 20201, pp. 188–197, doi: 10.25 165/j.ijabe.20 201 304.197.

[20] P. Kaushik, "Classification of indian states and union territories based on their soil macronutrient and organic carbon profiles," *bioRxiv*, 2020, doi:10.1101/2020.02.10.930586.

[21] A. K. Patel, J. K. Ghosh, and S. U. Sayyad, "Fractional abundances study of macronutrients in soil using hyperspectral remote sensing," *Geocarto International*, vol. 37, no. 2, pp. 474–493, Feb. 2022, doi:.

[22] U. Sadowska, I. Domagała-Świątkiewicz, and A. Żabiński, "Biochar and its effects on plant–soil macronutrient cycling during a three-year field trial on sandy soil with peppermint (mentha piperita l.). part i: Yield and macro element content in soil and plant biomass," *Agronomy*, vol. 10, no. 12, p. 1950, Dec. 2020, doi:10.3390/agronomy10121950.

[23] S. Shiwakoti, V. D. Zheljazkov, H. T. Gollany, M. Kleber, B. Xing, and T. Astatkie, "Macronutrient in soils and wheat from long-term agroexperiments reflects variations in residue and fertilizer inputs," *Scientific Reports*, vol. 10, no. 1, pp. 1–9, May 2020, doi:10.1038/s41598-020-60164-6.

[24] R. Madhumathi, T. Arumuganathan, and R. Shruthi, "Soil npk and moisture analysis using wireless sensor networks," in *2020 11th International Conference on Computing, Communication and Networking Technologies (ICCCNT)*, Jul. 2020, pp. 1–6, doi: 10.1109/ICCCNT49 239.2020.9 225 547.

[25] L. Burton, K. Jayachandran, and S. Bhansali, "The 'real-time' revolution for in situ soil nutrient sensing," *Journal of The Electrochemical Society*, vol. 167, no. 3, p. 037569, Jan. 2020, doi:10.1149/1945-7111/ab6f5d.

[26] J. Lisuma, E. Mbega, and P. Ndakidemi, "Influence of tobacco plant on macronutrient levels in sandy soils," *Agronomy*, vol. 10, no. 3, p. 418, Mar. 2020, doi:10.3390/agronomy10030418.

[27] J. F. Alves, S. L. Donato, P. E. Donato, J. D. Silva, and B. V. Guimarães, "Establishment of sufficiency ranges to determine the nutritional status of 'gigante' forage cactus pear–macronutrients," *Journal of Agricultural Science*, vol. 11, no. 18, pp. 213–221, 2019, doi:10.5539/jas.v11n18p213.

[28] D. N. Carvalho, C. Gonçalves, J. M. Oliveira, D. S. Williams, A. Mearns-Spragg, R. L. Reis, and T. H. Silva, "A design of experiments (doe) approach to optimize cryogel manufacturing for tissue engineering applications," *Polymers*, vol. 14, no. 10, p. 2026, 2022, doi:10.3390/polym14102026.

[29] J. Outeiro, W. Cheng, F. Chinesta, and A. Ammar, "Modelling and optimization of machining of ti-6al-4v titanium alloy using machine learning and design of experiments methods," *Journal of Manufacturing and Materials Processing*, vol. 6, no. 3, p. 58, 2022, doi:10.3390/jmmp6030058.

[30] C. M. Dragan and D. Lelea, "Thermal design optimization of the printed circuit board through area reduction," *Heat Transfer Engineering*, vol. 43, no. 3–5, pp. 248–256, 2021, doi:10.1080/01457632.2021.1874654.

[31] B. W. Chong, R. Othman, R. P. Jaya, M. R. M. Hasan, A. V. Sandu, M. Nabiałek, B. Jeż, P. Pietrusiewicz, D. Kwiatkowski, P. Postawa, and M. M. A. B. Abdullah, "Design of experiment on concrete mechanical properties prediction: A critical review," *Materials*, vol. 14, no. 8, p. 1866, 2021, doi:10.3390/ma14081866.

[32] S. Chandra and O. Prakash, "Performance optimization of a microchannel heat sink using taguchi design of experiments," *Solid State Technology*, vol. 63, no. 2s, pp. 1–11, 2020, accessed: October 1, 2024. [Online]. Available: http://www.solidstatetechnology.us/index.php/JSST/article/view/2451

[33] E. V. Arcieri, S. Baragetti, and Božić, "Application of design of experiments to foreign object damage on 7075-t6," *Procedia Structural Integrity*, vol. 31, pp. 22–27, Mar. 2021, doi:10.1016/j.prostr.2021.03.005.

[34] D. A. Guerra-Zubiaga and K. Y. Luong, "Energy consumption parameter analysis of industrial robots using design of experiment methodology," *International Journal of Sustainable Engineering*, vol. 14, no. 5, pp. 996–1005, 2021, doi:10.1080/19397038.2020.1805040.

[35] L. Román-Ramírez and J. Marco, "Design of experiments applied to lithium-ion batteries: A literature review," *Applied Energy*, vol. 320, p. 119305, 2022, doi:10.1016/j.apenergy.2022.119305.

[36] I. Yarici and Y. Öztürk, "Analysis of an inverted square srr via design of experiment (doe) approach," *Journal of Electrical Engineering*, vol. 72, no. 4, pp. 273–277, 2021, doi:10.2478/jee-2021-0038.

[37] A. Rodríguez, L. Martínez, L. Miranda, L. Peña-Parás, S. Cruz, D. Maldonado, and M. Rodríguez-Villalobos, "Simulation of texture geometries to optimize tribological properties," pp. 145–156, November 3-5 2021, accessed: October 1, 2024. [Online]. Available: http://ieomsociety.org/monterrey2021/papers/34.pdf

[38] W. J. Dacay, E. B. Amante, J. A. Bacal, and L. Ryan, "Npk soil nutrients identification for corn using optical transducer with mobile application," *Journal of Critical Reviews*, vol. 7, no. 15, pp. 6434–6444, 2020, accessed: October 1, 2024. [Online]. Available: https://www.researchgate.net/publication/369659854_NPK_SOIL_NUTRIENTS_IDENTIFICATION_FOR_CORN_USING_OPTICAL_TRANSDUCER_WITH_MOBILE_APPLICATION

[39] S. Manickam, "Iot-based soil condition monitoring framework," Oct. 14 2020, doi:10.2139/ssrn.3711616.

[40] K. Golicz, S. H. Hallett, R. Sakrabani, and G. Pan, "The potential for using smartphones as portable soil nutrient analyzers on suburban farms in central east china," *Scientific Reports*, vol. 9, no. 1, pp. 1–10, 2019, doi:10.1038/s41598-019-52702-8.

[41] G. Lavanya, C. Rani, and P. GaneshKumar, "An automated low cost iot based fertilizer intimation system for smart agriculture," *Sustainable Computing: Informatics and Systems*, vol. 28, p. 100300, 2020, doi:10.1016/j.suscom.2019.01.002.

[42] Z. Hou, Y. Tang, C. Li, K. J. Lim, and Z. Wang, "The additive effect of biochar amendment and simulated nitrogen deposition stimulates the plant height, photosynthesis and accumulation of npk in pecan (carya illinoinensis) seedlings," *AoB Plants*, vol. 12, no. 4, 2020, doi:10.1093/aobpla/plaa035.

[43] V. Budinski and D. Donlagic, "All silica micro-fluidic flow injection sensor system for colorimetric chemical sensing," *Sensors*, vol. 21, no. 12, p. 4082, 2021, doi:10.3390/s21124082.

[44] H. Yuan, T. Tsai, H. Wang, Y. Chien, C. Chen, C. Chu, C. Ho, P. Chu, and C. Chen, "A manual and portable centrifuge combined with a paper-based immunoassay for myocardial infarction diagnosis," *Chemical Engineering Journal*, vol. 409, p. 128131, 2021, doi:10.1016/j.cej.2020.128131.

[45] A. Guterstam, H. H. Kean, T. W. Webb, F. S. Kean, and M. S. Graziano, "Implicit model of other people's visual attention as an invisible, force-carrying beam projecting from the eyes," in *Proceedings of the National Academy of Sciences*, vol. 116, no. 1, 2019, pp. 328–333, doi:10.1073/pnas.1 816 581 115.

[46] S. Huang, S. Luo, Y. Yang, T. Li, Y. Wu, Q. Zeng, and H. Huang, "Determination of optical rotation based on liquid crystal polymer vortex retarder and digital image processing," *IEEE Access*, vol. 10, pp. 8219–8226, 2022, doi:10.1109/ACCESS.2022.3141224.

[47] M. Yukhymenko, A. Artyukhov, R. Ostroha, N. Artyukhova, J. Krmela, and J. Bocko, "Multistage shelf devices with fluidized bed for heat-mass transfer processes: Experimental studies and practical implementation," *Applied Sciences*, vol. 11, no. 3, p. 1159, 2021, doi:10.3390/app11031159.

[48] G. Gani and F. Qadir, "A robust copy-move forgery detection technique based on discrete cosine transform and cellular automata," *Journal of Information Security and Applications*, vol. 54, p. 102510, 2020, doi:10.1016/j.jisa.2020.102510.

[49] H. N. Winata, R. Noguchi, A. Tofael, and M. A. Nasution, "Prediction of microalgae total solid concentration by using image pattern technique," *Journal of the Japan Institute of Energy*, vol. 98, no. 5, pp. 73–84, 2019, doi:10.3775/jie.98.73.

[50] P. K. Mall, P. K. Singh, and D. Yadav, "Glcm based feature extraction and medical x-ray image classification using machine learning techniques," in *2019 IEEE Conference on Information and Communication Technology (CICT)*, 2019, pp. 1–6, doi: 10.1109/CICT48 419.2019.9 066 263.